ARCHIVE OF MECHANICAL ENGINEERING

DOI: 10.24425/ame.2024.149185 2024, Vol. 71, No. 1, pp. 73–85

Andrzej MITURA [1], Krzysztof KECIK [1]

Energy recovery from a system with double magnet. Analytical approach

Received 13 November 2022, **Revised** 24 January 2024, **Accepted** 1 February 2024, **Published online** 8 March 2024

Keywords: energy recovery, double magnet, nonlinear electromechanical coupling, analytical approach

The main goal of the research presented in this paper is to find an analytical solution for an electromagnetic energy harvester with double magnet. A double magnet configuration is defined as a structure in which two magnets, either attracting or repelling, are positioned at a constant distance from each other. Analytical dependencies that govern the shape of electromechanical coupling coefficient curves for various double magnet configurations are provided. In the subsequent step of the analysis, resonance curves for its vibrations and the corresponding recovered energy were determined for the selected dual magnet settings using the harmonic balance method. These characteristics enabled us to ascertain the optimal resistance and estimate the maximum electrical power that can be harvested from the vibrations of the double magnets.

1. Introduction

In the 20th century, human civilization experienced rapid development, largely due to the widespread use of fossil fuels for energy production. However, relying on these energy sources in the long term has led to numerous issues, such as climate change. Nowadays, people are increasingly conscious of the dangers associated with burning fossil fuels, and there is a growing recognition of the necessity to overhaul the global energy system. This sentiment is supported by research on the perspectives of young people, as presented in the article [1].

During the research, the opinions of young people from South-Eastern Poland were analyzed. The most important conclusions indicate that 78% of respondents

✉ Andrzej MITURA, e-mail: a.mitura@pollub.pl

[1]Lublin University of Technology, Faculty of Mechanical Engineering, Department of Applied Mechanics, Lublin, Poland

see a relationship between carbon dioxide emissions (an anthropogenic factor) and climate change. Additionally, 69.8% of respondents express a willingness to reduce consumption. One method to reduce energy consumption is by recovering it from operating devices. For instance, a self-driven crane undergoes two basic work cycles: lifting and lowering the load. The concept of energy recovery from the lowering cycle is presented in the paper [2].

In the kinematic chain, an additional DC generator is integrated. The recovered energy, in the form of electricity, is used to heat the resistor of a solid particle filter. Another idea can be applied to buildings. Their roofs could be covered with special panels designed to recover energy from rain. A piezo roof harvesting system is described in [3]. Raindrops possess mass, velocity, and their motion is characterized by frequency. When the drops impact the panel, variable forces are generated, which the piezoelectric panel can convert into electricity.

The examples presented above pertain to objects created by humans. However, humans themselves can also be sources of recoverable energy. A fundamental activity is walking. As people walk, they carry backpacks, handbags, etc. Inside these items, an energy harvester can be installed. Put et al. proposed a special construction of a backpack [4]. Inside it, there is a load plate connected with an electromagnetic rotary harvester via a strap system. During the walk, the vibrations of the carried load are converted by the harvester into electricity. A more versatile solution is an electromagnetic harvester with a levitating magnet [5]. This device can be placed in a backpack, attached to a leg, etc. The principle of operation of this harvester is very simple, as the induced current is generated by the motion of the magnet relative to the induction coil. In a classic electromagnetic harvester, there is one movable magnet, known as a single-pole case. An alternative approach involves using a complex movable magnetic structure, which may consist of multiple magnets and spacers. This variant is referred to as a multi-pole case. Comparative studies of single and multi-pole cases can be found in [6, 7]. The authors of these works employ numerical or experimental studies to determine which case allows for the recovery of more energy. The presented results indicate that the solution with a multi-pole structure is more effective. However, systems with multi-poles are not very well-described from an analytical perspective. The complexity of such systems gives rise to some challenges, such as the existence of high-order power functions. The main aim of this study was to propose procedures that could be utilized in analytical calculations.

This paper focuses on the analysis of the so-called double magnet system. A double magnet comprises two magnets, either attracting or repelling, with a constant distance between them. The first crucial aspect of this study involves determining the electromechanical coupling coefficient for the double magnet. This is presented in Section 2, where functions describing the coefficient curves are proposed. In the next section, the model of the electromagnetic harvester is displayed. The electromechanical coupling coefficient introduces strongly nonlinear terms into the mathematical model. The second significant aspect of this research was

establishing the analytical solution and assessing its accuracy (Section 3). Finally, the obtained results are summarized in the Conclusions section.

2. Electromechanical coupling coefficient for double magnet

The basic components of an electromagnetic energy harvester consist of a double magnet system and an inductive coil (see Fig. 1). The forces generated between these elements are contingent upon the electromechanical coupling coefficient, a topic addressed in this section.

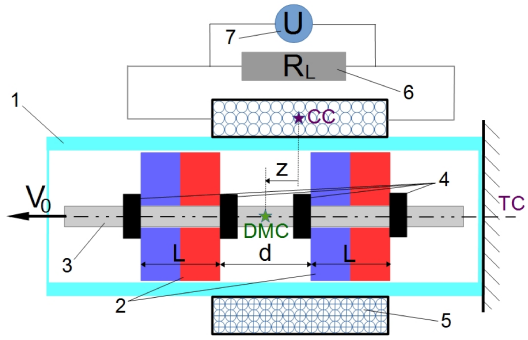

Fig. 1. Configuration of experimental setup for identifying the electromechanical coupling coefficient. 1 – transparent tube, 2 – two separate permanent magnets, 3 – threaded rod, 4 – nuts, 5 – induction ring coil, 6 – resistor, 7 – voltmeter, TC – tube clamping, CC – coil center, DMC – double magnet structure center, d – constant distance between both magnets, L – single magnet length, V_0 – constant speed of double magnet motion, z – coordinate describing the relative motion of double magnet (DMC) versus coil (CC)

The double magnet system comprises two identical single magnets, a threaded rod, and nuts. The single magnets are neodymium rings with a length of 20 mm and diameters: inner 5 mm, outer 20 mm. They are made of neodymium NdFeB N38 material with residual flux density 1.26 T. A rod is threaded through the holes of the magnets. Depending on the configuration of the magnets' poles, they can either attract (NS-NS) or repel (NS-SN) each other. Nuts are employed to maintain a constant distance d between the magnets. Both the rod and nuts are constructed from non-magnetic material, specifically brass. The characteristic point of the double magnet is referred to as the DMC (double magnet center). This point is located halfway between the individual magnets ($d/2$). The trajectory of motion for this point is a straight line, as the double magnet is housed inside a tube. Meanwhile, the second crucial element of the harvester is mounted outside the tube: the induction coil. The key geometric parameters of the coil are its length (50 mm), inner diameter (28 mm), and outer diameter (42 mm). The wire with a diameter of 0.14 mm wound within the coil (12 740 turn of winding) results in a

resistance and inductance of $R_C = 1.15$ kΩ and $L_C = 1.46$ H, respectively. The harvested energy is dissipated in an additional resistor with resistance R_L.

To ascertain the electromechanical coupling coefficient, this system should be set up, for instance, within a strength-testing machine. The tube, and consequently the coil, should remain stationary. Therefore one end of the tube was clamped (as indicated by the TC symbol in Fig. 1), while the double magnet was connected to the machine traverse and it underwent motion. It is advisable to employ a triangular signal to generate motion at the DMC point, as this will maintain a constant magnet speed of $\pm V_0$. Throughout testing, measurements should be taken for both the distance z between the DMC and CC (coil center) points, and the voltage U. Both measurement signals were taken from the displacement sensor of the strength-testing machine and the voltmeter, respectively. Sample measurement results are provided in the work [8]. Both of these signals were used in electromechanical coupling coefficient α identification. Based on paper [8], the relationship between the electromechanical coupling coefficient α and the induced voltage can be written in following form:

$$\alpha(z) = \frac{U}{V_0}. \tag{1}$$

The result of the calculation is a trend $\alpha(z)$. This indicates that the value of the electromechanical coupling coefficient α depends on the relative position z of the double magnet and the coil. Here lies the issue: for a different distance between single magnets d, a different curve of electromechanical coupling process $\alpha(z)$ is obtained. An alternative to multiple measurements of trend $\alpha(z, d)$ is described in [8]. In this concept, a measurement is made between one single magnet and a coil. However, the coefficient α for double magnet system is calculated from the superposition of two separate interactions of individual magnets and a coil. This necessitates establishing a relationship between the position of the centers of the right and left magnets relative to the coil center. The new variables are defined as follows:

$$z_1 = z + \frac{d+L}{2}, \tag{2a}$$

$$z_2 = z - \frac{d+L}{2}, \tag{2b}$$

where: L is the length of a single magnet, d is constant distance between the two-single magnet, and z is the distance between the DMC and CC points. The trend of the electromechanical coupling coefficient for the single magnet-coil interaction (α_1 or α_2) can be described by a polynomial function [8]. Using the new coordinates (2), the following equations were defined to separately describe the interactions between the right and left magnets and the coil:

$$\alpha_1 = \lambda_1 z_1 + \lambda_3 z_1^3 + \lambda_5 z_1^5 + \lambda_7 z_1^7 + \lambda_9 z_1^9 + \lambda_{11} z_1^{11} + \lambda_{13} z_1^{13} + \lambda_{15} z_1^{15}, \tag{3a}$$

$$\alpha_2 = \lambda_1 z_2 + \lambda_3 z_2^3 + \lambda_5 z_2^5 + \lambda_7 z_2^7 + \lambda_9 z_2^9 + \lambda_{11} z_2^{11} + \lambda_{13} z_2^{13} + \lambda_{15} z_2^{15}. \tag{3b}$$

The electromechanical coupling coefficient for a double magnet can be determined using the superposition principle. However, it should be noted that double magnets may have different pole configuration. Two cases can be distinguished when magnets will be attracted (α_a) or repelled (α_r). For these two different double magnet configurations, the coupling coefficient is calculated from the relationship:

$$\alpha_a = \alpha_1 + \alpha_2 \,, \tag{4a}$$

$$\alpha_r = \alpha_1 - \alpha_2 \,. \tag{4b}$$

Equations (4a) or (4b) allow us to determine the trend of the electromechanical coupling coefficient versus z and d parameters. The coefficients of the polynomial model for the single magnet-coil interaction, necessary for calculations are presented in Table 1. The resulting curves of the electromechanical coupling coefficient for the double magnet system are shown in Fig. 2.

Table 1. Values of polynomial coefficient (3)

Coefficient	Value
λ_1	2.758×10^{3} Nsm^{-2}
λ_3	-3.521×10^{6} Nsm^{-4}
λ_5	1.889×10^{9} Nsm^{-6}
λ_7	-5.412×10^{11} Nsm^{-8}
λ_9	8.916×10^{13} Nsm^{-10}
λ_{11}	-8.462×10^{15} Nsm^{-12}
λ_{13}	4.298×10^{17} Nsm^{-14}
λ_{15}	-9.044×10^{18} Nsm^{-16}

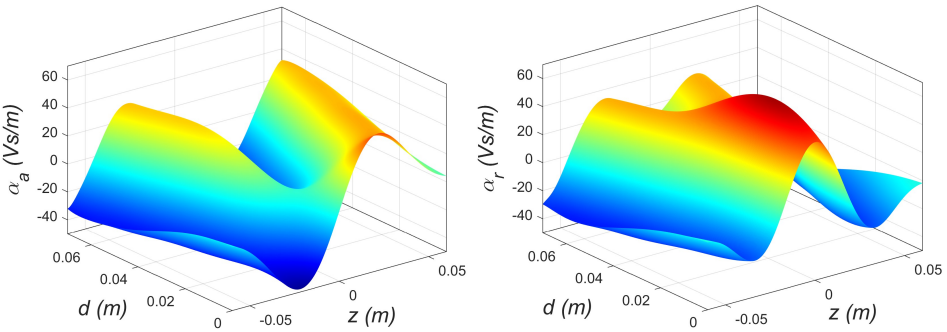

Fig. 2. Characteristics of electromechanical coupling coefficient for double magnet system, where magnets are (a) attracted or (b) repulsed

The applied methodology allows for the analytical determination of curves $\alpha(z, d)$ for all variants of the double magnet system. When analyzing the obtained results, attention should be given not only to the maximum or minimum values, but also to their positions. The natural initial position of the double magnet (equilibrium in the harvester) relative to the coil may occur at $z = 0$ m, where the positions of the DMC and CC points overlap. In this case, a double magnet with attracting magnets will be ineffective. For small vibrations around initial position ($z = 0$ m) the electromechanical coupling coefficient will be close to zero, resulting in negligible recovered energy. To increase the level of recovered energy, it is suggested to shift the double magnet's equilibrium relative to the coil.

On the other hand, for a double magnet with repulsive magnets, the situation is reversed. At $z = 0$ m the initial configuration of the DMC and CC points is optimal. For small vibrations, the maximum coupling coefficient exists at $z = 0$ m and a magnet distance of $d = 0.018$ m (Fig. 3a – blue series). However, for larger vibrations, the value of the α_r coefficient would quickly decrease. With a larger distance d, the maximum values of α_r will be slightly smaller, but in a wider range of z variable, the coefficient α_r will have high values (e.g., Fig. 3a – red series). Changing the shape of the electromechanical coupling coefficient curve quantitatively and qualitatively affects the efficiency of energy recovery. In addition to differences in the maximum current/voltage value, the type of responses obtained may be different, i.e., single harmonic response when the value of α_r is constant or multi-harmonic for variable value of α_r. Taking this into account, it was decided that the case with $d = 0.05$ m may be more practical and will be considered further in this paper.

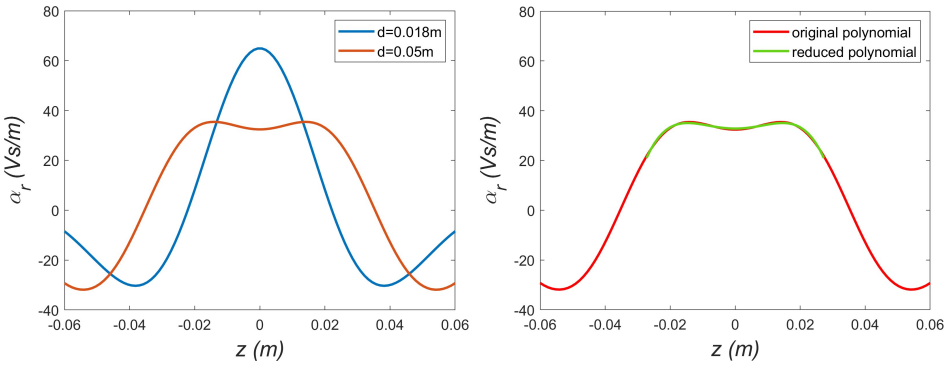

(a) (b)

Fig. 3. Selected curves of $\alpha_r(z, d)$: (a) comparison for different distance d and (b) modeling using a reduced polynomial

The red curves in Fig. 3a ranging from $z = -0.02$ m to $z = 0.02$ m exhibit a coupling coefficient value close to 34 Vs/m. As an initial approximation, it can be assumed that this coefficient remains constant value within this range. The

full description using Eq. (4b) is intricate and challenging to employ in analytical methods. In article [9], the use of simplified model is proposed. For a narrower range of displacement, a lower-order polynomial can be applied for local approximation. For z from −0.03 to 0.03 m, data from the original polynomial model were fitted using the reduced polynomial:

$$\alpha(z) = \alpha_0 + \alpha_2 z^2 + \alpha_4 z^4. \tag{5}$$

The effect of local approximation using the reduced model is evident in Fig. 3b (green series). The new, simpler polynomial reproduces the original shape well and it can be applied in analytical investigation. The obtained coefficients of polynomial (5) are presented in Table 2.

Table 2. Values of polynomial coefficient (5)

Coefficient	Value
α_0	32.82 Nsm^{-1}
α_2	2.118×10^4 Nsm^{-3}
α_4	-4.978×10^7 Nsm^{-6}

3. Analytical considerations of electromagnetic harvester dynamic

The system depicted in Fig. 1 has been expanded to create the complete structure of an electromagnetic energy harvester (Fig. 4). Many researchers have employed magnetic levitation suspension in systems of this type. However, altering the settings of the permanent or moving magnets can impact magnetic interactions and suspension characteristics [10]. Modifying the structure of the tested double magnet, such as pole configuration or distance (d), results in a change in the electromechanical coupling coefficient curve and, consequently, alerts the magnetic suspension characteristic. Considering changes in suspension characteristics may

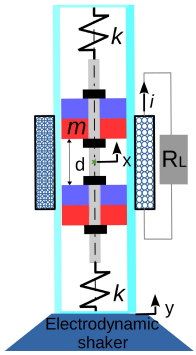

Fig. 4. Scheme of an electromagnetic harvester

introduce ambiguity in the analysis of the coupling coefficient's impact. Therefore, this design proposes a classic coil spring [11], in which modifications in the double magnet will not change the suspension characteristic. Consequently, two linear springs with stiffness coefficient k are placed inside the tube. They serve as the suspension for a double magnet with a mass m, which is the sum of the masses of all components: two magnets, threaded rod and nuts. The linearity of the suspension means that the gravitational force is balanced by the preload of these springs. Consequently, the gravitational force only causes a static deflection $z_S = mg/(2k)$. Ultimately, the gravitational effect and the constant response offset caused by it are not included in the system model.

In the damping model, it is assumed that the sources of damping are air resistance and mechanical damping in the springs' material. Friction between magnets and tube is neglected, because there is a gap between the magnets and the tube and changing the type of suspension does not cause forced emphasis of the magnets on the tube wall, which is typical for magnetic suspension [10]. The maximum speeds of the moving magnet reach up to approximately 2 m/s. Therefore, the applied viscous damping model with coefficient c should be sufficient.

The electromagnetic harvester was affixed to an electrodynamic shaker, generating the kinematic excitation. The periodic excitation y induces vibrations in the double magnet, with their absolute motion described by the coordinate x. The coil facilitates the conversion of some mechanical energy from these vibrations into electricity. As a result, current i flows in the coil circuit. An additional resistor R_L is responsible for receiving the recovered energy. The equation for the relative motion of the double magnet, expressed as $z = x - y$, can be written as:

$$m\ddot{z} + 2kz + c\dot{z} + \alpha(z)i = m\ddot{y}. \tag{6}$$

For systems where the coil inductance L is much smaller than the resistance R, the inductance can be neglected [9]. Then, the current can be calculated from the relationship:

$$i = \frac{\alpha(z)\dot{z}}{R}, \tag{7}$$

where R is a total resistance, i.e., the sum of the resistance of the coil R_C and the resistor R_L. Substituting Eq. (5) and (7) into (6), the final form of the differential equation of motion was obtained:

$$m\ddot{z} + 2kz + c\dot{z} + \frac{\left(\alpha_0 + \alpha_2 z^2 + \alpha_4 z^4\right)^2}{R}\dot{z} = m\ddot{y}, \tag{8}$$

where the term including reduced polynomial $\alpha(z)$ generates nonlinearity in the harvester system. In general, this term induces additional damping, which is associated with the process of energy recovery. This phenomenon is referred as electrical damping. The description of excitation term arises from the assumption that the

motion of electrodynamic shaker armature would be controlled based on a constant value of acceleration amplitude. Then, the kinematic excitation signal can be expressed as:

$$y = -\frac{a}{\omega^2}\sin\omega t \quad \text{or} \quad \ddot{y} = -a\sin\omega t, \tag{9}$$

where a is the mentioned constant acceleration amplitude and ω is excitation frequency.

The analytical solution for system (8) was determined using the harmonic balance method [12]. The first-order approximation was taken in the following form:

$$z = B_1\cos\omega t + B_2\sin\omega t = B\sin(\omega t + \phi). \tag{10}$$

The appropriate transformation using the harmonic balance method led to determination of relationship for the vibration amplitude of the double magnet $B^2 = B_1^2 + B_2^2$. This relationship took the form of an 18th order polynomial. However, the exponents are only even and by introducing a new variable $C = B^2$, the order of the polynomial can be reduced to the following form:

$$\beta_0 + \beta_1 C + \beta_2 C^2 + \beta_3 C^3 + \beta_4 C^4 + \beta_5 C^5 + \beta_6 C^6 + \beta_7 C^7 + \beta_8 C^8 + \beta_9 C^9 = 0, \tag{11}$$

where the parameters are defined as:

$$\begin{aligned}
\beta_0 &= -m^2a^2,\\
\beta_1 &= \left(2k - m\omega^2\right)^2 + c^2\omega^2 + \frac{\omega^2}{R^2}\alpha_0^4 + \frac{2c\omega^2}{R}\alpha_0^2,\\
\beta_2 &= \frac{\omega^2}{R^2}\alpha_0^3\alpha_2 + \frac{c\omega^2}{R}\alpha_0\alpha_2,\\
\beta_3 &= \frac{\omega^2}{2R^2}\alpha_0^2\alpha_2^2 + \frac{\omega^2}{2R^2}\alpha_0^3\alpha_4 + \frac{c\omega^2}{4R}\alpha_2^2 + \frac{c\omega^2}{2R}\alpha_0\alpha_4,\\
\beta_4 &= \frac{\omega^2}{8R^2}\alpha_0\alpha_2^3 + \frac{9\omega^2}{16R^2}\alpha_0^2\alpha_2\alpha_4 + \frac{5c\omega^2}{16R}\alpha_2\alpha_4,\\
\beta_5 &= \frac{\omega^2}{64R^2}\alpha_2^4 + \frac{11\omega^2}{64R^2}\alpha_0^2\alpha_4^2 + \frac{7\omega^2}{32R^2}\alpha_0\alpha_2^2\alpha_4 + \frac{7c\omega^2}{64R}\alpha_4^2,\\
\beta_6 &= \frac{17\omega^2}{128R^2}\alpha_0\alpha_2\alpha_4^2 + \frac{5\omega^2}{128R^2}\alpha_2^3\alpha_4,\\
\beta_7 &= \frac{7\omega^2}{256R^2}\alpha_0\alpha_4^3 + \frac{39\omega^2}{1024R^2}\alpha_2^2\alpha_4^2,\\
\beta_8 &= \frac{35\omega^2}{2048R^2}\alpha_2\alpha_4^3,\\
\beta_9 &= \frac{49\omega^2}{16384R^2}\alpha_4^4.
\end{aligned}$$

Based on Eq. (11), resonance curves were determined with respect to excitation frequency ω and resistance R. The following parameters were used for the calculations: $m = 0.18$ kg, $c = 1$ Ns/m, $k = 350$ N/m, $a = 15$ m/s^2, ω ranging from 50 to 80 rad/s, R_L ranging from 0 to 5 kΩ, and the coupling coefficient from Table 2. The obtained amplitudes $B = C^{0.5}$ are shown in Fig. 5a. Whereas, the current i was reconstructed from Eq. (7):

$$i(\omega t + \phi) = \frac{\alpha_0 + \alpha_2 \left(B \sin(\omega t + \phi)\right)^2 + \alpha_4 \left(B \sin(\omega t + \phi)\right)^4}{R} B\omega \cos(\omega t + \phi), \quad (12)$$

where $\omega t + \phi$ can change from 0 to 2π. Based on the maximum current value $i_{\max}$ found from the calculations using Eq. (12), the maximum instantaneous electrical power $P_{\max}$ can be estimated:

$$P_{\max} = R_L \, i_{\max}^2 \, . \quad (13)$$

The electrical power obtained in this way is shown in Fig. 5b.

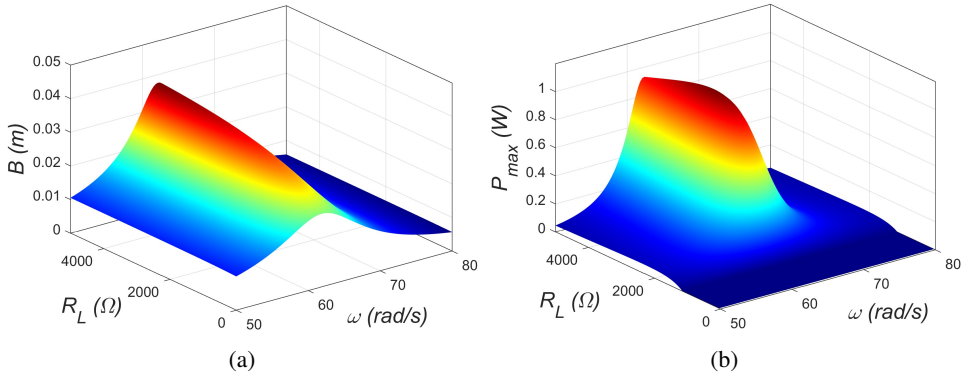

Fig. 5. Results of analytical calculations: (a) obtained $B(\omega, R_L)$ and (b) estimated $P_{\max}(\omega, R_L)$

The resonance curves for magnet vibrations show that an increase in load resistance leads to higher amplitudes of B. This can be attributed to the fact that the resistance R is in the denominator of the term related to the energy recovery process in Eq. (8). A higher resistance means that the influence of this term is smaller, resulting in a lower so-called electrical damping. As a result, with lower electrical damping, the vibration amplitudes B may be larger. However, from the perspective of energy recovery effectiveness, finding the optimal resistance is required. Analyzing Eq. (13), it can be observed that the maximum power results from the current level $i_{\max}$ and the resistance value R_L. In Eq. (12), where $i_{\max}$ the load resistance R_L appears directly in the nominator $R = R_C + R_L$ and indirectly in the numerator, where amplitude B depends on electrical damping (as described in the trend from Fig. 5a above). The combined direct and indirect influence of R_L on the maximum electrical power resulted in a value of about 0.92 W, which was

obtained at the excitation frequency equal to the resonant frequency of 62.42 rad/s and the load resistance of 2.474 kΩ. This load resistance is more than twice as large as the coil resistance value of 1.15 kΩ.

Additional calculations were performed to establish the relationship between the optimal load resistance and mechanical damping. The obtained 3D characteristic $P_{\max}(c, R_L)$ for the resonance frequency $\omega = 62.42$ rad/s is presented in Fig. 6a. Based on the maximum power values for appropriate damping c, the optimal resistance values $R_{L,\text{opt}}$ were estimated, as shown in Fig. 6b. The observed trend $R_{L,\text{opt}} = f(c)$ reaches maximum values for $c \approx 1$ Ns/m. This trend for $c > 1$ corresponds with the known relationship for linear systems with a constant electromechanical coupling coefficient [13] – decreasing the optimal resistance with increasing damping c. Some similarities between both curves can be attributed to the fact that the applied coefficient model $\alpha(z)$ has values with small deviations from a constant value over a wide range. In this zone, for larger mechanical damping c, the optimal load resistance tends to approach the coil resistance. However, for $c < 1$, double magnet vibrations can be more pronounced, leading to larger deviations $\alpha(z)$ from the constant value. Consequently, a reversal in the trend was observed. For low mechanical damping, instead of increasing, $R_{L,\text{opt}}$ decreases. Another challenge arises in this zone. The level of vibration amplitudes B exceeds the range of z where the applied reduced polynomial approximates the electromechanical coupling coefficient curve effectively (see Fig. 3b). Therefore, this portion of the trend $R_{L,\text{opt}} = f(c)$ may be subject to certain limitations.

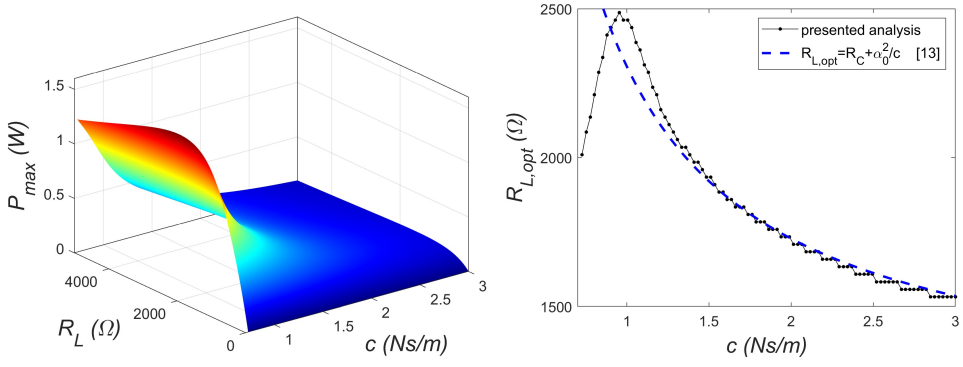

(a) (b)

Fig. 6. Curves $P_{\max}(c, R_L)$ for $\omega = 62.42$ rad/s (a) and the trend $R_{L,\text{opt}} = f(c)$ developed on their basis (b)

The final step of the analysis involved verifying the accuracy of the obtained results. Eq. (8) was implemented in a numerical model using Simulink software. Numerical simulations were conducted for a specific load resistance value ($R_L = 1$ kΩ) and then compared with the analytical results (Fig. 7).

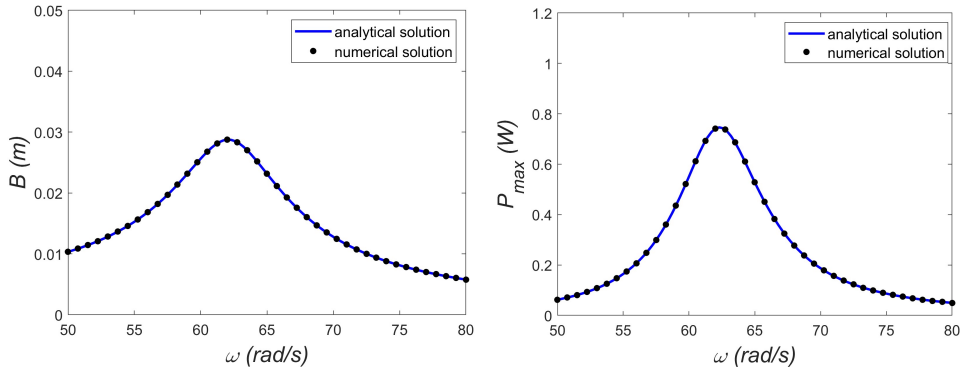

(a) (b)

Fig. 7. Comparison of analytical and numerical results: (a) double magnet vibration and (b) electrical power with $R_L = 1$ kΩ, $c = 1$ Ns/m

A comparative analysis of analytical and numerical calculations confirms a very good agreement between both sets of results. Negligibly small errors indicate that, in this case, the use of the first-order approximation in the harmonic balance method is sufficient.

4. Conclusions

This paper presents an analytical approach to modeling and testing an electromagnetic harvester with an oscillating magnet consisting of double magnets. The proper design of double magnets allows for the modification of the electromechanical coupling shape. The proposed identification procedure enables a quick analytical determination of this curve.

In this paper, the analysis was limited to only two parameters: load resistance and excitation frequency or load resistance and mechanical damping coefficient. Nevertheless, information about the optimal resistance, its dependence on mechanical damping, and the maximum power of recovered energy were specified for selected double magnet configurations. Note, that the coupling coefficient is a nonlinear function, the resonance curves remain linear.

The obtained instantaneous electrical power at the level of about 1W is highly promising. This underscores the necessity for further research into the possibility of modifying electromechanical coupling curves. The analytical approach employs a first-order approximation. The level of approximation error was verified numerically. For the amplitude vibration of the double magnet and the maximum electrical power, analytical and numerical curves are practically identical. Therefore, the obtained analytical solutions were deemed accurate, even though only a first-order approximation was used. In the future, analysis with a modified reduced polynomial adapted to larger vibrations is planned.

Acknowledgements

This research was financially supported by the National Science Center according to decision no. 2019/35/B/ST8/01068.

References

[1] M. Wozniak, K. Kud, A. Badora, and L. Wozniak. Electricity production and consumption perspectives in the opinion of the youth of South-Eastern Poland. *Energies*, 15:4776, 2022. doi: 10.3390/en15134776.

[2] J. Ocioszynski and P. Majewski. Energy recovery for reducing toxic exhaust emissions in selected energetic states of individual operating cycle in self-driven heavy machinery. *Archive of Mechanical Engineering*, 48(4):301–317, 2001.

[3] R. Di Leo, M. Viscaedi, F.P. Tuccinardi, and M. Visione. Numerical modelling of a piezo roof harvesting system: the right component selection. *Archive of Mechanical Engineering*, 64(2):257–282, 2017. doi: 10.1515/meceng-2017-0016.

[4] K. Fan, P. Xia, R. Li, J. Guo, Q. Tan, and D. Vei. An innovative energy harvesting backpack strategy thought a flexible mechanical motion rectifier. *Energy Conversion and Management*, 264:115731, 2022. doi: 10.1016/j.enconman.2022.115731.

[5] P. Carneiro, M.P. Soares dos Santos, A. Rodrigues, J.A.F. Ferreira, J.A.O. Simoes, A. Torres Marques, and A.L. Kholkin. Electromagnetic energy harvesting using magnetic levitation architectures: a review. *Applied Energy*, 260:114191, 2020. doi: 10.1016/j.apenergy.2019.114191.

[6] S.C. Kim, J.G. Kim, Y.C. Kim, S.J. Yang, and H. Lee. A study of electromagnetic vibration energy harvesters: design optimization and experimental validation. *International Journal of Precision Engineering and Manufacturing-Green Technology*, 6:779–788, 2019. doi: 10.1007/s40684-019-00130-4.

[7] B.C. Lee and G.S. Chung. Low-frequency driven energy harvester with multi-pole structure. *Journal of Mechanical Science and Technology*, 29(2):441–446, 2015. doi: 10.1007/s12206-015-0102-5.

[8] A. Mitura and K. Kecik. Investigation of electromechanical coupling characteristic of a double magnet system. *Materials Research Proceedings*, 30:55–60, 2023. doi: 10.21741/9781644902578-8.

[9] A. Mitura and K. Kecik. Analytical and numerical analysis of electromagnetic harvester with a nonlinear coupling. *Proceedings of the 29th International Congress on Sound and Vibration*, 29:426, 2023.

[10] A. Mitura and K. Kecik. Modeling and energy recovery from a system with two pseudo-levitating magnets. *Bulletin of the Polish Academy of Sciences Technical Sciences*, 70(4):e141721, 2022. doi: 10.24425/bpasts.2022.141721.

[11] M. Ostrowski, B. Blachowski, M. Bochenski, D. Piernikarski, P. Filipek, and W. Janicki. Design of nonlinear electromagnetic energy harvester equipped with mechanical amplifier and springs bumpers. *Bulletin of the Polish Academy of Sciences Technical Sciences*, 68(6):1373–1383, 2020. doi: 10.24425/bpasts.2020.135384.

[12] M.A. Razzak. A simple harmonic balance method for solving strongly nonlinear oscillators. *Journal of the Association of Arab Universities for Basic and Applied Sciences*, 21:68–76, 2016. doi: 10.1016/j.jaubas.2015.10.002.

[13] M. Mosch and G. Fischerauer. A comparison of methods to measure the coupling coefficient of electromagnetic vibration energy harvesters. *Micromachines*, 10(12):826, 2019. doi: 10.3390/mi10120826.